Technische Universiteit Delft

Spatiotemporal aeolian sediment transport variabilities at Oysterville (WA) beach

Anne Verheijen

TU Delft

Spatiotemporal aeolian sediment transport variabilities at Oysterville (WA) beach

by

Anne Verheijen

As additional thesis (CIE 5050)

At the Delft University of Technology

Thanks to Nick Cohn, who provided bed elevation data of SEDEX²'s research area

The data shown in this report can be found with DOI: 10.4121/uuid:2122d1af-6f61-435e-9635-3dc4f6837aef

Student number: 4234960
Project duration: July 1, 2016 – October 17, 2016
Thesis committee: Dr.Ir. Sierd de Vries, TU Delft
Dr. Roderik C. Lindenbergh, TU Delft
Dr. Sander E. Vos, TU Delft

TU Delft

Abstract

Aeolian sediment transport is an important factor in beach and dune system recovery after a storm. Global warming, causing sea level rise and more intense storms, makes insight in this process more and more important.

Changes in spatiotemporal variability of aeolian sediment transport as result of bar welding are studied in this paper, within the scope of SEDEX². The distinction between supply limited and transport limited transport is used as introduced by de Vries et al. in 2013. SEDEX² is a field campaign at Oysterville, Washington state, beach aimed to improve the understanding of beach-dune dynamics by testing the hypothesis that sediment supply to the backshore beach and dunes is dominated by the welding of intertidal sandbars to the shoreline. The main question in this aeolian study is therefore; "What is the influence of bar welding on spatiotemporal variability of the aeolian sediment transport gradients?". It is hypothesized that the total aeolian sediment transport to the dunes should increase after bar welding, because bar welding makes more sand available to be blown into the dunes. This means that more accretion should be seen in the dune area and more erosion in the intertidal area, where the sand bar has welded. In other words; a change in sedimentation erosion patterns should be seen. The expected increase in sediment transport, due to more supply indicates that the beach is hypothesized to be supply limited.

The main question can be split into three elements that need to be investigated. The first is whether the beach is transport or supply limited. The yearly averaged measured transport rates are compared to a Bagnold type of calculation to find an answer to this first part. Keeping track of the bar welding process is the second element. Certain transects will be monitored with GPS, by walking and driving Jet Skis, to capture the evolution of the beach. The third piece is measuring sedimentation erosion patterns at different stages in the bar welding process with a terrestrial laser scanner.

The hypothesis is concluded to be false; the investigated beach is transport limited instead of supply limited and that bar welding doesn't influence the spatiotemporal variability of the aeolian sediment transport gradients. The Bagnold type of calculation shows that the sand transport capacity to the dunes is the same order of magnitude as the actual yearly averaged observed sediment transport, indicating transport limited sediment transport. The sedimentation erosion patterns obtained at different stages in the bar welding process show no differences that cannot be explained by the wind direction and speed. This shows that hypothesis is false; the bar welding doesn't influence the spatiotemporal variability of the aeolian sediment transport gradients. Is has to be noted that sedimentation erosion patterns have been measured at three days, with different wind speed and direction. Therefore different wind speeds and directions can explain the differences in observed patterns, but there could be differences covered up by these effects.

Anne Verheijen
Delft, October 2016

Contents

1 Introduction

The dune system is an important factor in the Dutch sea defense, as it is in many other places in the world. Three processes determine the building/erosion rate of these dunes. First sediment transport driven by hydrodynamic processes, second aeolian sediment transport and lastly vegetation cycles. Global warming, causing sea level rise and more intense storms, makes insight in these processes more and more important, because the recovery of the beach and dune system depends on it.

The aeolian sediment transport was almost always, and still is often, calculated based on the work done by Bagnold Bagnold [1937], causing over predictions. In 2013 de Vries et al. introduced a new way of describing aeolian sediment transport on a beach. This new method took into account supply limited situations, meaning that the sediment transport is limited by the presence of erodible sand [de Vries et al., 2013]. In a supply limited case the transport capacity, calculated with a Bagnold type formula, is higher than the actual transport. This means that if the wind velocity increases, thus transport capacity, the amount of sand that is blown away remains the same. The Bagnold type of transport is redefined as transport limited, meaning that wind velocity is the limiting factor for transport. An increase in wind velocity also increases the actual transport in this case.

The variability in aeolian sediment transport on a beach with varying sediment supply has been measured during a 3 day campaign in the Netherlands [de Vries et al., 2014]. It was seen that the amount of sediment transport was significantly influenced by the availability, which was controlled by the tide. The situation was thus supply limited. The supply from the upper beach was relatively low due to sorting processes, shell fragments remained at the surface forming an armor layer, called armoring. The supply from the intertidal area was relatively large when it was exposed. In this area the armor layer is reworked. An aeolian sediment transport study has also been done at the Sand Motor during a 6 week long campaign [Hoonhout and de Vries, 2016]. In this research erosion was mainly seen in the intertidal area and armoring occurred on the dry beach, the sediment transport is supply limited.

Tide, fetch and beach profile (changes) are important factors for the spatiotemporal variability of the aeolian sediment transport, see figure 1.1. The beach profile can be split in three parts; the submerged part, intertidal area and the dry beach. The tide in combination with the beach profile creates an intertidal area. In this area the top layer of sediment is reworked, making it an important area of supply. Especially if the upper, dry, beach is supply limited, e.g. due to armoring. Tide also influences the fetch, with low water the fetch length is larger than with high water, see figure 1.1. Fetch is defined as the distance downwind from a boundary marking the transition from a non-erodible to an erodible surface. It affects the downwind sediment transport rate, transport increases exponentially, in ideal situations, with an increasing fetch length, up to the critical fetch [Delgado-Fernandez, 2010]. Sand can be non-erodible in the intertidal zone due to surface moisture. The influence of the submerged coastal profile lies in sediment supply to the backshore. Beach and dune growth requires onshore migration and welding of nearshore bars to get sediment supply for aeolian sediment transport to the dunes [Houser, 2012]. This bar welding will also influence the fetch by increasing the intertidal area.

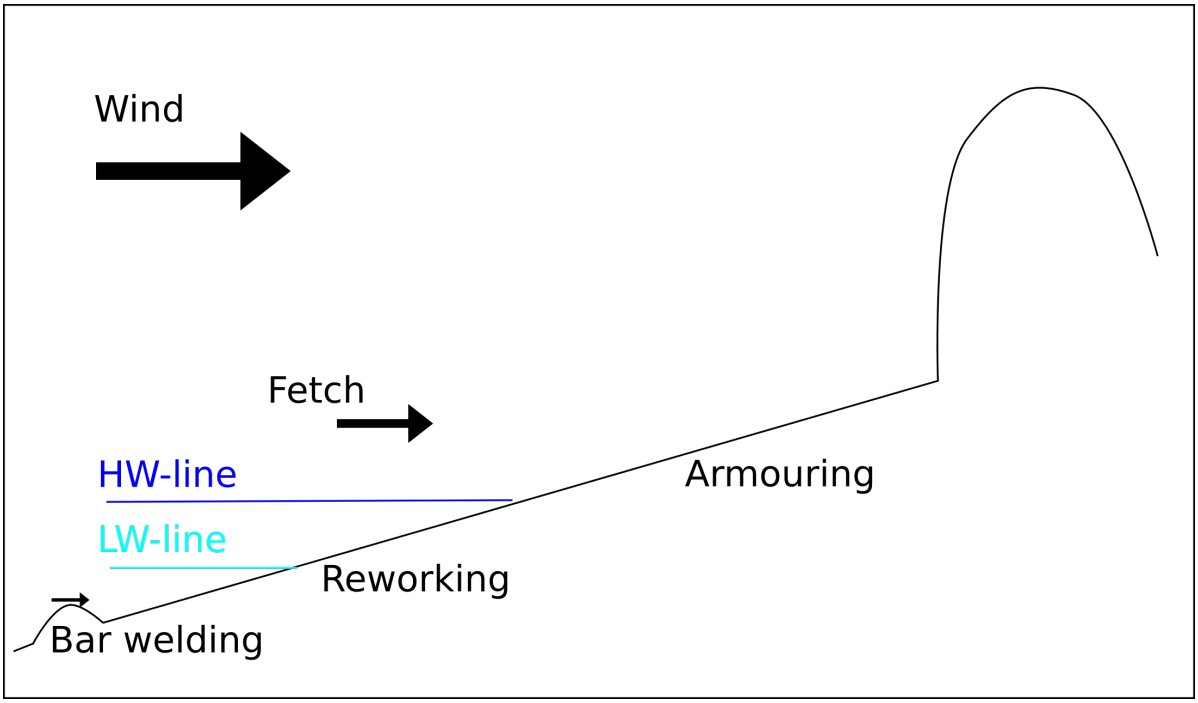

Figure 1.1: The processes important for spatiotemporal aeolian sediment transport variability are indicated; tide, fetch and beach profile (changes).

In this paper the change in spatiotemporal variability of aeolian sediment transport as result of bar welding is studied within the scope of Sandbar-aEolian-Dune EXchange Experiment (SEDEX²). SEDEX² is a 6 week field campaign conducted in the summer of 2016 by Oregon State University, financially supported by the National Science Foundation, NSF. It is done at a part of the beach in Oysterville, Washington State, on the Long Beach peninsula, see figure 1.2. The research area is characterized by a dissipative beach and long term progradation of the coastline, currently 3 to 4 meter per year [Ruggiero, 2013]. SEDEX²'s aim is to improve the understanding of beach-dune dynamics by testing the hypothesis that sediment supply to the backshore beach and dunes is dominated by the welding of intertidal sandbars to the shoreline. The main question of this paper therefore is; "What is the influence of bar welding on spatiotemporal variability of the aeolian sediment transport gradients?". It is hypothesized that the total aeolian sediment transport to the dunes should increase after bar welding, because bar welding makes more sand available. This means that more accretion should be seen in the dune area and more erosion in the intertidal area, where the sand bar has welded.

Figure 1.2: SEDEX² location, Oysterville in Washington State, is indicated with a red pushpin in the figure on the left. On the right a more detailed map of the area is shown. In that figure also Grays Harbor's offshore buoy and Toke Point are indicated, with green pushpins.

An important aspect for the main question is whether the aeolian sediment transport is supply or transport limited. The hypothesis of the main question is that the total sediment transport will be increased by the increase in availability, this indicates that the transport is hypothesized to be supply limited. If the situation on the beach is not supply limited but transport limited the influence of bar welding can be completely different. In that case the increase in availability, intuitively, doesn't matter for the total amount of sediment transported to the dunes, as long as the fetch length was already longer than the critical length. Another important aspect for determining the influence of the bar welding is how large the wind driven erosion/sedimentation rate of the beach and the intertidal area is before and after bar welding.

Summarizing; three things have to be determined to answer the main question, the transport regime, when bar welding happens and the sedimentation erosion patterns at different stages of bar welding. Determination whether the situation is supply or transport limited, the transport regime, will be done by comparing a type of Bagnold calculation with yearly averaged measured transport volumes at the field site. A limitation is that the chosen values for parameters in the formula are not verified with actual field measurements, the volume of sediment transported with certain wind speeds is not measured. The erosion and sedimentation rates on the beach and intertidal area will be determined with a terrestrial laser scanner (TLS). This method is limited by the amount of experience with applying it on beaches. To get some more insight in the suitability of the method reference measurements with GPS are done and the method is applied on a windless day. The bar welding process itself will be measured by doing GPS measurements every day.

2

Methodology

The methodology can be split into three elements. The first is determining whether the transport regime is supply or transport limited. Monitoring bar welding, the second element, is treated afterwards. The methodology is concluded by explaining the observation method of the sedimentation erosion patterns, the third element.

2.1. Transport regime

The regime of sediment transport will be determined, supply or transport limited, by comparing the transport capacity with the measured transport. The sediment transport capacity is the amount of transport if it is not limited by the presence of erodible sand. It will be calculated with measured wind velocities and formula 2.1. This formula is a combination of a Bagnold type formula with velocity threshold [Bagnold, 1937] and taking the wind direction into account with a sinus function. Note the negative sign in front of the sinus. This is a result of the orientation of the coast. Wind blowing to the east, between 180 and 360 degrees, will transport sand to the dunes.

$$q = \alpha * C_b * \frac{\rho}{g} * \sqrt{\frac{d}{D}}(u - u_t)^3 * -\sin(\theta) \qquad [\frac{kg}{m * s}] \tag{2.1}$$

$with$:

$\alpha = (\frac{0.174}{\log_{10}\frac{z}{k_0}})^3$ [−]

$k_0 = \frac{1}{30} * d$ [m]

$z = wind\ at\ height\ z\ above\ the\ bed = 0.5$ [m]

$C_b = 1.8$ ($based\ on\ grain\ size\ distribution\ width$) [−]

$\rho = density\ of\ the\ air \approx 1.225$ [$\frac{kg}{m^3}$]

$g = gravitational\ constant = 9.81$ [$\frac{m}{s^2}$]

$d = nominal\ grain\ size = 180 * 10^{-3}$ [m]

$D = reference\ diameter = 250 * 10^{-}3$ [m]

$u = wind\ speed$ [$\frac{m}{s}$]

$u_t = wind\ speed\ threshold\ for\ sediment\ movement = 4.5$ [$\frac{m}{s}$]

$\theta = wind\ direction$ [$degree$]

The average sediment transport capacity in a year can be calculated with measured wind data. Wind speed and direction measured from April 2005 until December 2014 at Toke Point, Washington State, see figure 1.2, is used [national data bouycenter]. The obtained total sediment transport capacity has to be multiplied with the density, 2650 kg/m³, and divided by the porosity, 0.4, of the sand to end up with a volume instead of a weight. This will be compared to the observed transport to the dunes, 10 to 20 m³ sand per running meter per year [Ruggiero, 2013]. The situation is transport limited if the observed transport is in the same order of magnitude as the calculated transport capacity, if it is smaller the situation is supply limited.

2.2. Bar welding

The bar welding process is recorded with GPS measurements with real time differential corrections (RTK). These are conducted every day around the lowest low tide by walking with GPS backpacks over specified transects, from the water line up to the dunes. The dunes are measured on a weekly interval to decrease trampling of the vegetation. The data collected on foot is supplemented for several transects by measurements done with Jet Skis equipped with echo sounders and GPS with RTK. This Jet Ski data is collected approximately every week, at the same day as the dune data. A transect is displayed in figure 2.1. All data collected on foot that deviates more than 2 meter on either side of the transect is not used. Every 0.1 meter a measurement is done. The GPS measurements on foot are in total done on 20 lines with a high interval and on 20 lines less frequent. Several lines run through the area investigated with the terrestrial laser scanner (TLS), see figure 2.1.

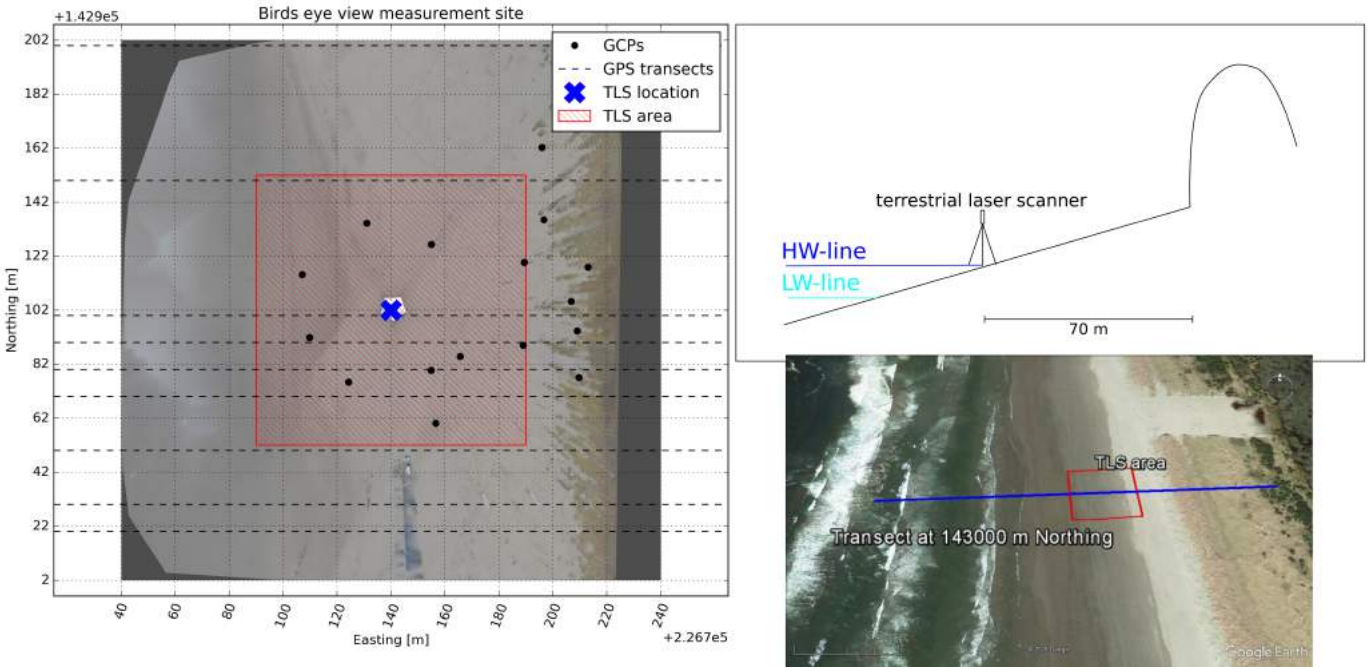

Figure 2.1: Birds eye view of the TLS measurement site on the left. In that figure on the right dunes can be seen in green and on the left darker sand of the intertidal area. The ground control points as used 29 August are indicated with black dots, also the TLS area and location are given. The upper right image shows a schematic cross section of the set-up of the TLS with respect to the dunes and the high and low water lines. On the lower left the GPS transect that goes through the middle of the TLS area is shown.

2.3. Sedimentation erosion patterns

The sedimentation erosion patterns are be obtained with use of a Riegl VZ2000 terrestrial laser scanner (TLS). First is explained how the TLS measurements are conducted. Afterwards is elaborated on the processing. During the scanning sequences the wind speed is measured at the test site with a station on top of the dune. An indication of the water line is obtained with tide measurements in Toke Point [NOAA], see figure 1.2, and wave buoy data measured near Grays Harbor [national data bouycenter], see figure 1.2. See appendix D for further elaboration.

2.3.1. Terrestrial Laser scanner measurements

The TLS, with camera on top for visual reference, is set upon a tripod, see figure 2.2, near the intertidal area, see figure 2.1. The height of the scanner on top of the tripod is a little over 3 meter. This location, near the intertidal area, is most interesting for both supply and transport limited aeolian transport. For supply limited transport it is interesting because during high tide sediment is reworked in the intertidal area and thus erodible sand is revealed when the tide retreats. For the transport limited case the gradients in transport are likely to occur not too far from the water line, the critical fetch is not yet reached in that case. This assumes wind blowing with an onshore component and sand not being too moisty to be blown away.

Figure 2.2: TLS set-up is shown on the left, TLS with camera on top on tripod. One ground control point is shown on the right.

TLS scan sequences are done on days with significant aeolian transport, 18, 29 and 30 August 2016. Scans have been done with a 7.5 minute interval except for the 18th, that day a 15 minute interval is used. Each scan a full circle, 360 degrees, is scanned from top to bottom. The laser footprint is 1 point every 2 cm at 50 meter range, assuming a flat surface. The camera on top is used to make pictures of this same 360.

For every scan the scanners position needs to be determined, using ground control points (GCP's) and RiScan-Pro software. Appendix B reveals that calculating the scanners position for every scan gives the best results, based on scans on a windless day. This research has been done on August 17th, therefore only windy days later than 17 August have been used. Calculating the scanners position means that the Northing, Easting and z coordinates and yaw, pitch and roll of the scanner are determined. The TLS software can be used to find for the scanner's coordinates and position based on the coordinates of the GCP's. Reflective circles are placed on wooden poles to create the GCP's, see figure 2.2. Their coordinates, center of the reflective circle, are measured with GPS RTK. Appendix B shows that the best result is obtained if the GCP's on all sides of the scanner are approximately the same distance away from it. This results in several fixed GCP's in the dunes and upper beach. The GCP's at the lower beach need to be placed and removed with each scan sequence due to safety concerns. The distance between the scanner and these points is less than for the fixed points because of tidal restrictions. Figure 2.1 shows the placement of GCP's at 29 August, in total 16 points are used.

The placement of the TLS has two practical issues, during a sequence it is desired that the scanner moves as little as possible and each sequence the scanner needs to be placed at approximately the same location for easier comparison of the sequences. The legs of the tripod are covered with compacted sand to prevent erosion around them, preventing movement of the TLS. The location of the TLS is indicated with a large piece of drift wood that is dug in. The scanner is installed at this location every day scans are made.

2.3.2. Processing terrestrial Laser scanner measurements

All the scans of a measuring sequence need to be processed to obtain results. The wanted results are a linear trend, squared correlation coefficient for this trend and standard deviations. The processing consists of three steps.

The first step of the processing is to filter the data. Reflectance is used to filter out dust flying around the laser scanner, points with reflectance lower than -20 dB are discarded. Also location and height are used to filter. A square of 100 by 100 m around the TLS is used as area of interest, everything outside that is removed. This is based on workability, the footprint of 2 cm on 50 m in combination with the scale of expected processes and on the GPS versus TLS measurements in the along shore direction in appendix A. Everything lower than 0 m height or higher than 5.7 m is removed, because it is unlikely to be part of the sand surface, based on the beach profile.

The remaining data is linearly interpolated on a grid of 3 by 3 cm, this is the second step. The spacing is chosen such that in theory in the far corners of the TLS area each grid point's height could be determined based on one measurement point. Closer to the scanner more points will be used to obtain the height of a grid point.

The third step is obtaining the desired results by processing the gridded data. The trend is found by linear regression through the z coordinates over time at each grid point. The squared correlation coefficient is between linear trend and height observations. The standard deviation is for the z coordinates at each grid point.

Coordinates measured with the TLS are compared to GPS RTK measurements in appendix A, revealing offsets of several centimeters. This indicates that it will be impossible to fit an accurate trend through the measurements if the observed trend is in the order of centimeters per scan sequence.

3

Results

The tripartite structure seen in chapter 2 is also applicable in this chapter. The first result shown concerns the transport regime; supply or transport limited aeolian sediment transport. The bar welding process is second and the third element is the sedimentation erosion patterns.

3.1. Transport regime

The calculated sediment transport capacity to the dunes is the same order of magnitude as the observed transport. An average sediment transport capacity of 13.6 cubic meter per year per running meter is obtained with the Bagnold type formula, 2.1. The observed transport to the dunes is 10 to 20 cubic meter sand per running meter per year [Ruggiero, 2013]. The situation is thus transport limited.

The transport limited situation is supported by visual observations in the field, see figure 3.1. It is clear that close to the suitcases a lot of scour has occurred and further away from the scanner not a lot happened. Close to the cases the wind field is disturbed by their presence. This disturbance causes local accelerations. Acceleration sets erosion in motion if the transport is transport limited. Higher velocity means more transport in that case and an increase in transport results in erosion. That the transport is transport limited around the cases can be concluded from this argumentation. It has to be noted that a much higher wind velocity is able to transit a supply limited case to a transport limited case by eroding the armor layer, revealing the better erodible layer below. If the accelerations around the suitcases are large enough to transit a possibly supply limited case to a transport limited case no conclusion can be drawn about the transport regime far away from the cases based only on the suitcase experiment.

Figure 3.1: Laser scanner suitcases before scanning sequence at 29-08 and 2 hours later.

3.2. Bar welding

One transect of the daily GPS measurements is shown in figure 3.2, it runs through the middle of the area that is analyzed with the TLS, 143000 m Northing. In this figure can be seen that the bar welding process takes place during the whole experiment, from the beginning to the end bars are migrating on shore. It can be seen that the area in front of the TLS area is developing more and more into a berm, just as the TLS area itself. This continues bar welding means that during the experiment more and more sand becomes available to be transported.

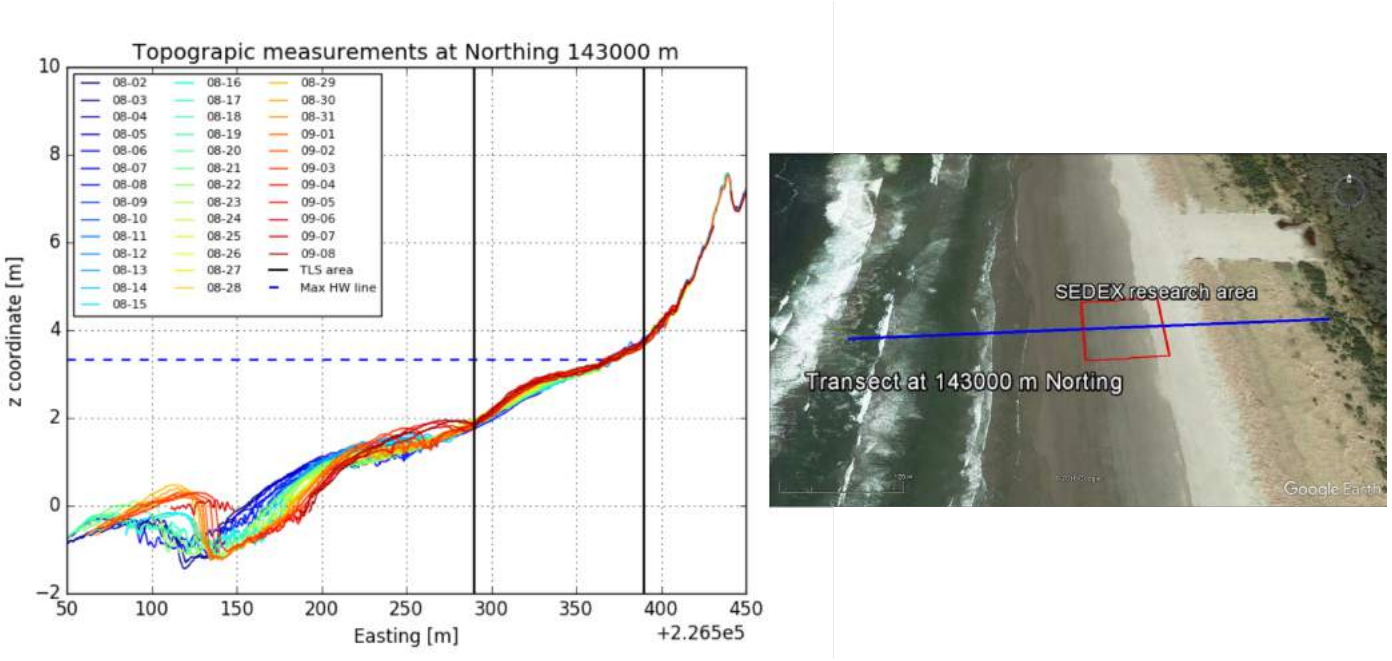

Figure 3.2: One transect of the topographic measurements done every day with GPS is shown on the left. This transect runs through the middle of the area that is analyzed with the TLS. The highest high water line is indicated with a horizontal dashed blue line, the height is based on appendix D. The borders of the TLS area are indicated with two vertical solid lines.

The changes in ground elevation are very small above the highest high water line in figure 3.2, see appendix D for derivation of this line. This could be explained by the fact that the wind speed in the measurement period is not often high enough to move sediment, see appendix C. The threshold for sediment movement was set on 4.5 m/s in the Bagnold formula, formula 2.1. In the field significant sediment transport was observed around 6.0 m/s. The direction during the high wind velocity events is also not beneficial for large growth of the upper beach. Two hundred and seventy degrees would mean cross shore sediment transport, during the wind events the direction is much more along shore, see appendix C.

The TLS measurements also show bar welding and not a lot of changes above the highest high water line. In figure 3.3 the TLS measurements are shown for the same transect, at 143000 m Northing. These elevations are obtained by averaging over the scan sequences, thus averaging over a day of measurements. In figure 3.4 the trend over the whole observation period, from 08-08 to 09-06 can be seen. This trend is obtained with a linear regression through the z coordinates over time at each grid point. Also the squared correlation coefficient, between linear trend and observations, is shown.

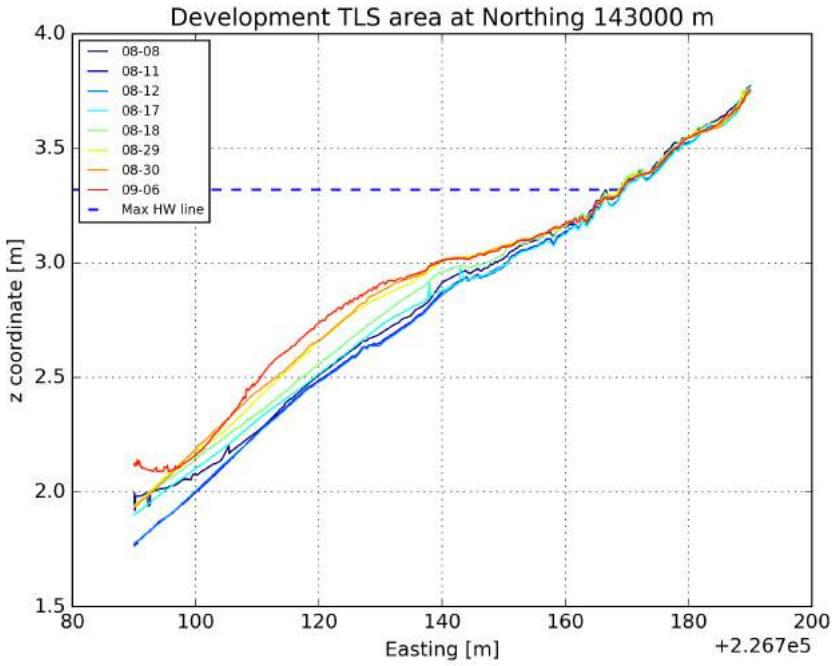

Figure 3.3: One transect of the TLS measured bed elevation, averaged over a whole scan sequence. The displayed transect has the same coordinates as the transect shown in figure 3.2. The transect is also indicated in figure 3.4. The highest high water line is indicated with a horizontal dashed blue line, the height is based on appendix D.

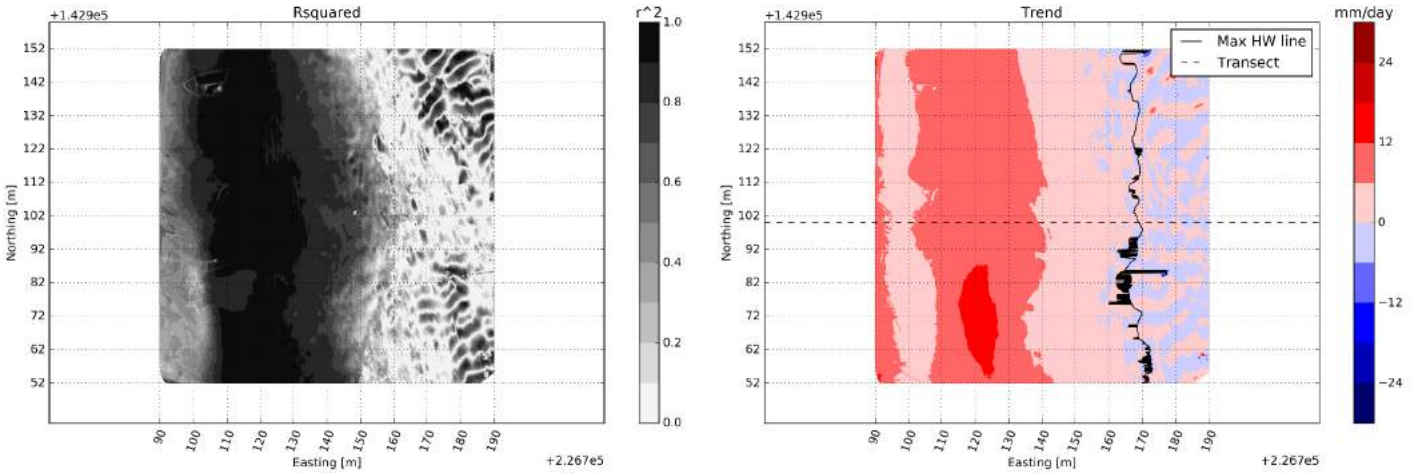

Figure 3.4: Trend and squared correlation coefficient for the linear trend observed between 08-08 and 06-09. The transect shown in 3.3 is indicated with a dashed black line in the trend figure, on the right. The highest high water line is indicated in this figure with a solid black line, the height is based on appendix D. Left of the highest high water line is the intertidal area.

3.3. Sedimentation erosion patterns

Three measuring sequences have been conducted on windy days after the finalization of the measuring routine on 17 August, see paragraph 2.3. The details of these sequences are shown in table 3.1 and the results are shown in figure 3.6. Figure 3.5 shows the evolution of one transect in time for each measuring sequence. See appendix C for more detail on the measured wind speed and direction measured at the test site. The trend, shown in figure 3.6, is obtained by linear regression through the z coordinates over time at each grid point. The squared correlation coefficient is between linear trend and observations. The standard deviation is for the z coordinates at each grid point. The results of the measuring sequences will be discusses separately below and then the similarities and differences will be addressed.

Date	Time high water (GMT)	Start time (GMT)	End time (GMT)	Avg. wind direction	Avg. wind speed	Number of scans
18-08	21:18	22:47	2:47	314 degree	7.1 m/s	17
29-08	19:24	20:47	0:47	182 degree	6.6 m/s	32
30-08	20:12	22:50	1:50	153 degree	6.8 m/s	24

Table 3.1: Details of measurement sequences. Wind speed and wind direction are based on appendix C.

3.3.1. August 18

August 18 the measuring sequence started right at high water, causing water inside the TLS area for several scans. These scans gave unrealistic results at the location of the water and are therefore removed. The processing is thus started right at the first scan without water in the TLS domain.

In figure 3.5 quite some scatter around the actual bed elevation can be seen, but also erosion can be distinguished. A lot of lines are visible in this figure, even at places where no erosion or accretion is seen, indicating scatter around the actual elevation, see e.g. around 170+2.267*10^5 m Easting on 18 August. The scatter can also be seen in the magnitudes of the standard deviations, shown in figure 3.6 for the whole TLS area. For all three days a zoom on the region near the high water line is made. Mainly erosion is seen in that zoom and also seaward of it, for the 18^{th}. This is also seen in the trend analysis shown in figure 3.6.

The borders of an area containing aeolian platforms are visible in the lower right hand corner of the results in figure 3.6. In the framework of SEDEX² platforms measuring wind speed, direction, saltation, moisture content, etc. have been placed. The area around these platforms has been bordered by ropes. These ropes wiggled around in the wind, which is visible in the standard deviation and the trend plot in figure 3.6.

Trend features, e.g. ripples or sedimentation erosion patterns, are absent below the high water line, see figure 3.6. Below the high water line only a larger area with erosion is seen on the 18^{th}. This area has low correlation coefficients, but not zero. Large ripple like features are seen at the whole beach above the high water line. They are running South West South to East North East, or vice versa, at the upper beach and West to East, 90 degrees, at the lower dry beach. In the field is observed that the bed forms at the lower part of the dry beach were up to several centimeters big, at the higher part, near the dune, the features grew larger, up to 10 cm.

3.3.2. August 29

On the 29^{th} the scan sequence started also just after the sea was out of the area, approximately one and a half hour after high water.

Figure 3.5 shows that above the high water line erosion took place and a little bit of accretion is seen around 12.5+2.2681*10^5 m Easting, for August 29. Also in figure 3.6 erosion near the high water line is seen, with a small strip of accretion onshore of it. Scatter around the actual bed level is also seen for this day, both in figure 3.5 and 3.6. Near the dunes ripple shaped patterns are observed, but not at the lower part of the beach. The ripples are oriented at 120 degrees, North West North to East South East. Below the high water line only larger area sedimentation and erosion, with low correlation coefficients, is found. In the trend and the standard deviation plot the aeolian area borders can be found again, see figure 3.6.

3.3.3. August 30

The high water line had retreated from the TLS domain for approximately an hour on the 30th before the measurement sequence started. The sequence started two and a half hours after high water.

A large spot with accretion is seen in figure 3.5 on this day, around 15+2.2681*10^5 m Easting and a small area with erosion is seen offshore of this accretion. Figure 3.6 also reveals a little bit of erosion near the high water line in the South, with a strip of accretion onshore of it. The accretion pattern is more significant than the day before. Ripple shaped patterns are shown over the whole beach above the high water line. They are at 90 degrees, West to East, at the whole beach. The height of the ripples is observed to be the same as on the 18th. Below the high water line only larger area sedimentation and erosion, with low correlation coefficients, is found. The borders of the aeolian area can be seen in the standard deviation and trend analysis, in figure 3.6.

3.3.4. Similarities and differences

Similarities and differences between the measuring sequences will be briefly discussed in this paragraph.

The starting time, with respect to the tide, is the same for 18 and 29 August. At 30 August the sequence is started approximately an hour later.

In all three measuring sequences ripple shape features are seen at the upper part, East, of the beach, but their orientation differs. These features are smaller and only seen on the 18th and 30th on the lower dry beach. It is clear from figure 3.6 that bigger trends are combined with higher squared correlation coefficients for all three sequences.

No significant trends are observed on the 29th and 30th below the high water line, correlation coefficients are nearly zero. For the 18th this is a bit higher. Just above the high water line erosion is seen on 29 and 30 August, onshore of this erosion sedimentation is seen.

Figure 3.6 shows that the standard deviations of the three sequences are not the same magnitude, on the 18th the biggest standard deviations are seen, followed by the 30th and then 29 August. The wind speed was the highest on 18 August, then August 30 and the least on the 29th, see table 3.1.

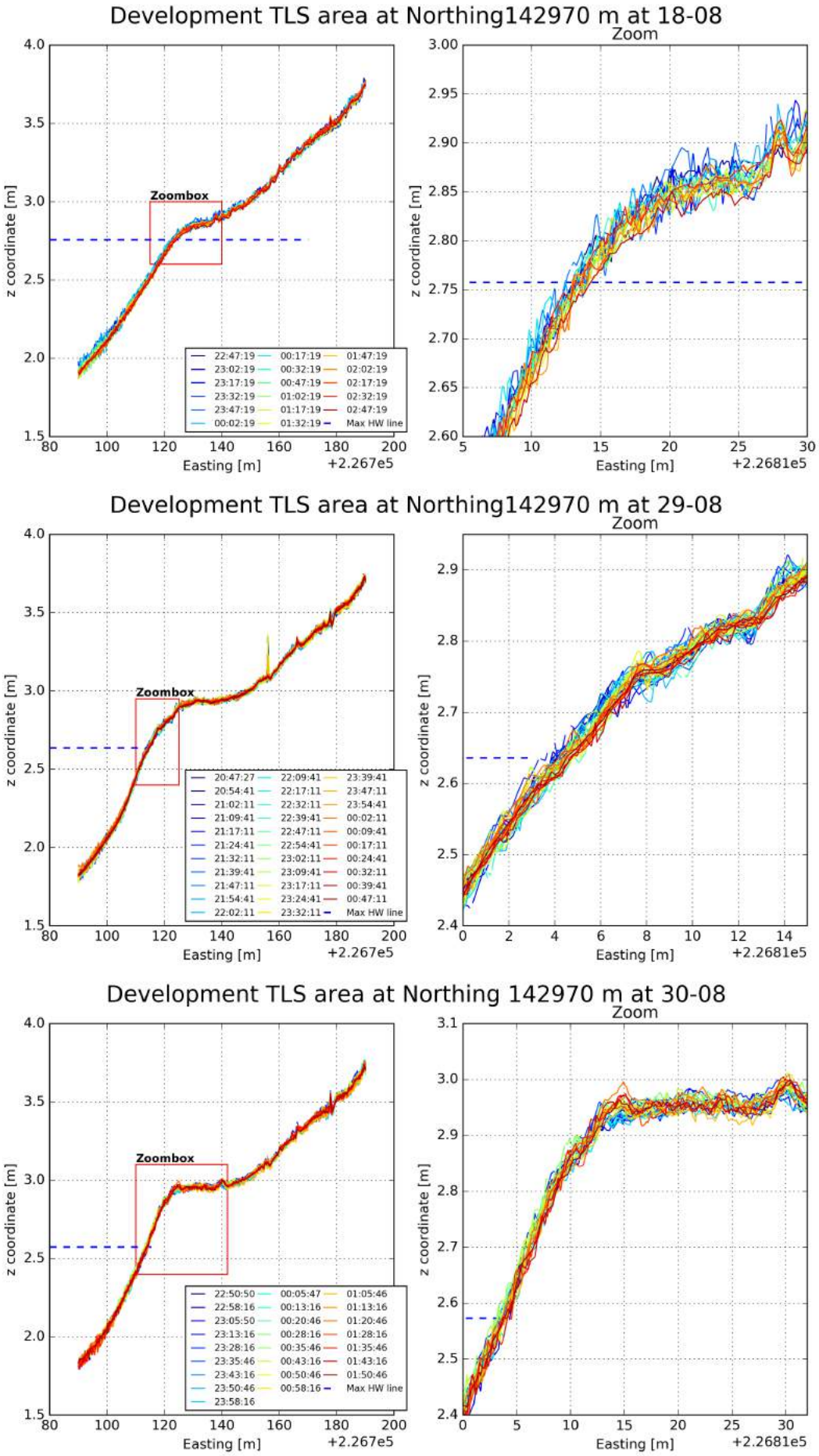

Figure 3.5: Bed elevation of one transect obtained with TLS, given for each scan in sequences. The location of this transect is 142970 m Northing and is also indicated in figure 3.6. On the left the whole transect is shown and a zoom in is shown on the right. The zoom box is indicated in the pictures on the left.

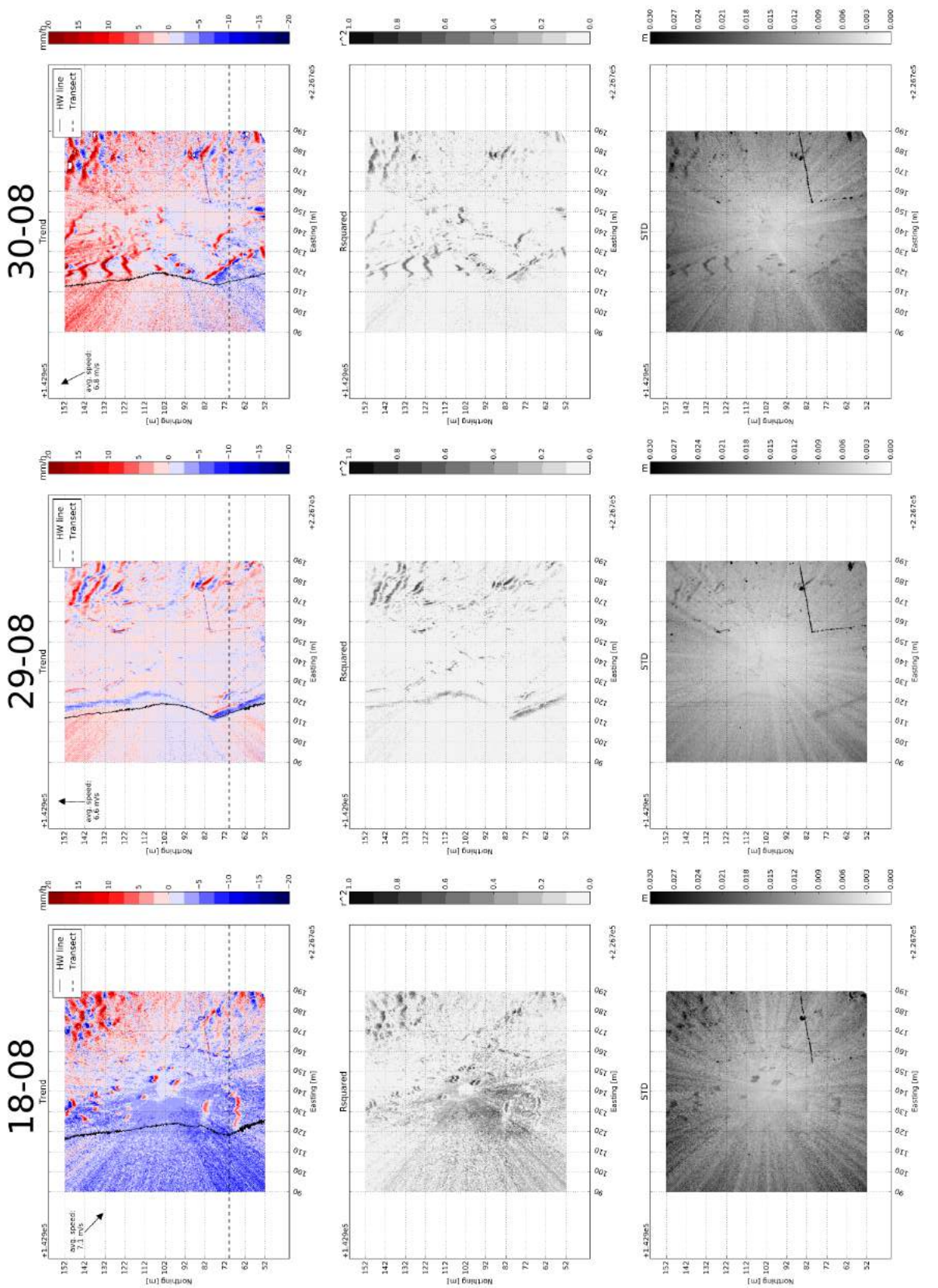

Figure 3.6: Trend, squared correlation coefficient and standard deviation for 18-08, 29-08 and 30-08. In the trend figure the high water line is indicated with a solid black line, the transect shown in 3.5 is given with a dashed black line. Left of this high water line is the intertidal area. The arrow indicates the average wind direction as measured at the test site and the average wind speed is given next to it.

4

Discussion

The measured wind direction, calculated high water line and difference in standard deviation shown in chapter 3 give rise to some discussion about their origin or correctness. This is discussed in this chapter.

The wind direction measured at the test site, shown in appendix C, seems to be incorrect when it is compared to human observation and ripple orientation. On the 30th the wind direction observed in the field was purely to the North, 180 degrees, instead of the measured 150 degrees. This purely north direction also corresponds better to the direction the ripples on the lower dry beach seem to move. They are oriented at 90 degrees, see paragraph 3.3, and thus orthogonal to the human observed wind direction. A reason why the ripples on the upper dry beach are not oriented 90 degrees could be that they still had to adjust to the wind direction. Those ripples are bigger in size, see paragraph 3.3, and thus slower in adjusting to the wind direction. On the 29th the measured wind direction is north, almost 180 degrees, but in the field a South West South wind was observed. The ripples are also orthogonal to that direction. The wind measured on the 18th is from a direction of approximately 315 degrees, West North West. The wind direction observed in the field was more North West North, again corresponding to the direction of most of the ripple shaped features.

The high water lines shown in chapter 3 are not very precise. They are based on a calculation, shown in appendix D, that makes use of tide measurements in a bay, Toke Point, see figure 1.2, and wave measurements some distance north of the test site, near Grays Harbor, see figure 1.2. It can be seen in figure 3.6 that the high water line is lower than the erosion pattern. This erosion pattern is likely to be caused by erosion of (fine) sediment that is brought in by the tide. Therefore it would be more likely if the high water line would have been a bit higher. The same can be said about 30 August. However, the water lines can still be used as approximations to give insight in the influence of the tide if it is kept in mind that they are not exact.

The standard deviations are larger if the wind speeds are higher, see paragraph 3.3, probably because the TLS shakes more on the tripod. The biggest standard deviation is seen for 18 Augustus, the day with the most wind, and the smallest for the 29th, day with the least wind. This gives rise to the expectation that the standard deviation is related to shaking of the TLS due to wind and wind gusts. It is also seen in that paragraph that the correlation coefficients are relatively low, especially with low trends. This can be explained by the large standard deviations, also observed in the transect plots in figure 3.5. A trend needs to be large to obtain a good correlation coefficient if there is a lot of variation around the trend.

5

Conclusion

The main question, hypothesize and the validity of this hypothesize will be discussed in this chapter.

The main question is “What is the influence of bar welding on spatiotemporal variability of the aeolian sediment transport gradients?”. It was hypothesized that the total aeolian sediment transport to the dunes should increase after bar welding, because bar welding makes more sand available. This indicates a supply limited situation at the beach. This means that more accretion should be seen in the dune area during wind events and more erosion in the intertidal area, where the sand bar has welded.

The Bagnold type calculation shows that the sand transport capacity to the dunes is the same order of magnitude as the actual observed yearly averaged sediment transport, see paragraph 3.1. This means that the sediment transport regime is on average not supply limited, as hypothesized, but transport limited. The transport capacity is the same as the actual transport, thus the transport is not limited by the presence of erodible sand.

Wind direction, wind speed and sequence starting time could explain the spatial differences in sedimentation erosion patterns between the sequences, observed in paragraph 3.3. A lot of erosion is seen offshore of the TLS on 18 August. On the 29^{th} it is mainly observed around the high water line and just a bit of accretion is seen just onshore of the erosion area. At 30 August this erosion and accretion pattern is not seen along the whole high water line, only seen in the South, and the width of the accretion band is larger. The timing of the scan sequences with respect to the tide can explain the difference in erosion between 29 and 30 August. On the 30^{th} the tide had already retreated for a longer time and a lot of erosion could have happened already. Furthermore, the direction of the wind is more along shore/offshore on the 30^{th} with respect to the 29^{th}, this could explain that on August 30 more accretion is seen. The difference between the 30^{th} and August 18 can be explained by the different wind direction. More erosion is seen on the 18^{th} and the wind direction is onshore for that day, instead of along shore/offshore. This means that the fetch starts in the intertidal area, which gives erosion in that area. The wind speed on the 18^{th} is on average 0.5 m/s larger than on 29 August, this could explain that a lot more erosion is seen on 18 August.

Paragraph 3.2 reveals that the bar welding process is advanced further during the measurements at 29 and 30 August than at the 18^{th}, however no differences in behavior are observed between the scan sequences in paragraph 3.3 that cannot be explained by the wind direction, speed and start time of the sequence, as explained in the previous paragraph. This is again an indication of the transport limited situation; the additional availability doesn't influence the transport volume. In other words; the bar welding doesn't influence the spatiotemporal variability of the aeolian sediment transport gradients and the hypothesis is thus false.

It has to be noted that the wind has been very mild during the experiment, the wind signal can be seen in appendix C. This results in 3 measuring sequences and the bar welding being the process that is dominantly present. More measurement sequences could have made it possible to eliminate the wind direction and speed influence on the behavior of the sedimentation and erosion patterns. Now different wind speeds and directions can explain the differences but there could be differences covered up by these effects.

6

Recommendations

Several recommendations are done in this chapter to improve the research done in this paper and possibly future researches. They are based on the discussion of the results, see chapter 4, and the conclusion, see chapter 5.

It is recommended to do measurements at same location in a period with more wind and higher wind velocities to increase the signals, because in this research the wind has been mild. This is likely to increase the correlation coefficients, which makes it easier to conclude about observed patterns. Moreover, more wind events raises the likelihood to obtain sequences with approximately the same wind speed and direction at different stages in the bar welding process. This will make it possible to eliminate the influence of wind direction and wind velocity.

Other improvements on this research would be to measure at more stages in the bar welding process and in several welding sequences with different characteristics. In this research two stages in one sequence are measured, at 18 August and 29 and 30 August. It could be thought of that other stages in the process differ more and thus different sedimentation erosion patterns could be observed. The speed and volume of the bar welding could also result in differences in the patterns; this could be captured if multiple welding sequences are measured.

It is observed in chapter 4 that higher wind velocities show higher standard deviations, due to movements of the TLS on the tripod. It is therefore recommended to make use of more sturdy mountings in the future, especially if wind velocities are higher than seen in this research and/or with more gusts. This could for instance be obtained by jacking down the tripod used in this research. The height of the TLS above the ground would also decrease by this measure, meaning that the investigated area should decrease as well.

The TLS set-up can also be improved with a better solution to prevent subsidence of the tripod's legs. Calculating the scanner's position in each scan has been used to cope with the settling of the legs in this research, see also appendix A. If just one scan position is determined for the whole sequence accuracies could increase. This is only possible if the tripod doesn't move any more. One solution could be to make big wooden plates with notches and place the tripod in the notches. With a bigger surface to stand on the sand subsidence will be less.

The sediment transport at the beach observed in this research is transport limited and bar welding is not influencing the spatiotemporal variability of the aeolian sediment transport gradients, see chapter 5. This raises the question if the influence of bar welding is substantial in case of a supply limited case. A recommendation is thus to do the same research at a beach that is supply limited and see whether the hypothesis is true in that case.

Bibliography

R. Bagnold. The transport of sand by wind. *Geographical Journal*, pages 409–438, 1937.

I. Delgado-Fernandez. A review of the application of the fetch effect to modelling sand supply to coastal foredunes. *Elsevier*, 2010.

B. Hoonhout and S. de Vries. Aeolian sediment transport at the sand motor mega nourishment. *Aeolian Research*, 2016.

C. Houser. Synchronization of transport and supply in beach-dune interaction. *Progress in Pyshical Geography*, 2012.

NOAA. (Consulted at: 09-25-2016). URL: `https://tidesandcurrents.noaa.gov/`.

NOAA national data bouycenter. (Consulted at: 09-25-2016). URL: `http://www.ndbc.noaa.gov/`.

P. Ruggiero. Morphodynamics of prograding beaches. *Coastal Dynamics Conference*, 2013.

H. Stockdon. Empirical parameterization of setup, swash and runup. *U.S. Elsevier*, 2006.

S. de Vries, J. van Thiel de Vries, L. van Rijn, S. Arens, and R. Ranasinghe. Aeolian sediment transport in supply limited situations. *Elsevier*, 2013.

S. de Vries, S. Arens, M. de Schipper, and R. Ranasinghe. Aeolian sediment transport on a beach with a varying sediment supply. *Elsevier*, 2014.

A

GPS VS TLS

A.1. Introduction

The terrestrial laser scanner's (TLS) measurements are compared to GPS measurements in this appendix. GPS measurement accuracies have been studied well. They are within several centimeters, horizontally a bit less than vertically. The deviation between GPS measurements and TLS observations are studied with increasing range from the scanner in along shore and cross shore direction. The main question for this appendix is "How do the observations done by the TLS compare to measurements done with GPS?". The first sub question is "Are the deviations between TLS and GPS different in along shore direction with respect to the cross shore direction?". "Does the difference between TLS and GPS increase with distance from the scanner?" is another sub question. The last one refers to the processing method "Are there differences between coordinates obtained with one and multiple scan positions?".

The hypothesis for these questions is that the deviations between TLS and GPS measured coordinates scatter around a certain value, comparable to the GPS accuracy, and then, at a certain distance from the scanner, start to increase with distance. This behavior is expected for both cross and along shore direction and for a single and multiple scan positions. It is thus hypothesized that the direction and number of times the scanners position is determined will not influence the deviations between GPS and TLS measured coordinates.

A.2. Methodology

Comparing GPS measurements with the TLS observations requires them to be at (almost) the same spots. Wooden sticks with reflective tape are constructed and put into the ground to deal with this challenge. These wooden sticks are approximately 4 centimeters wide and 20 centimeters high, the reflective tape part is 10 cm long. The sticks are put into the ground with the reflective tape out of the ground and the non-reflective part completely in the sand. In a scan the reflectance of the tape is higher than the surroundings and therefore the sticks are easy to distinguish.

The sticks are first in along shore direction placed and then in cross shore direction, to decrease the number of required sticks, see figure A.1 for the locations relative to TLS. For both directions 5 scans are made. The reflectance of each scan, visualized as 3D data cloud, is used to distinguish manually points in the middle of the stick faces. The coordinates of these points are written down and compared to the GPS coordinates, again measured in front of the sticks, in the middle.

Multiple and single solutions for the scanner's position are used for both directions. Multiple solutions means that the location of the scanner is determined for each scan individually based on the ground control points (GCPs), see paragraph 2.3 for more explanation on how the scanners position is found.

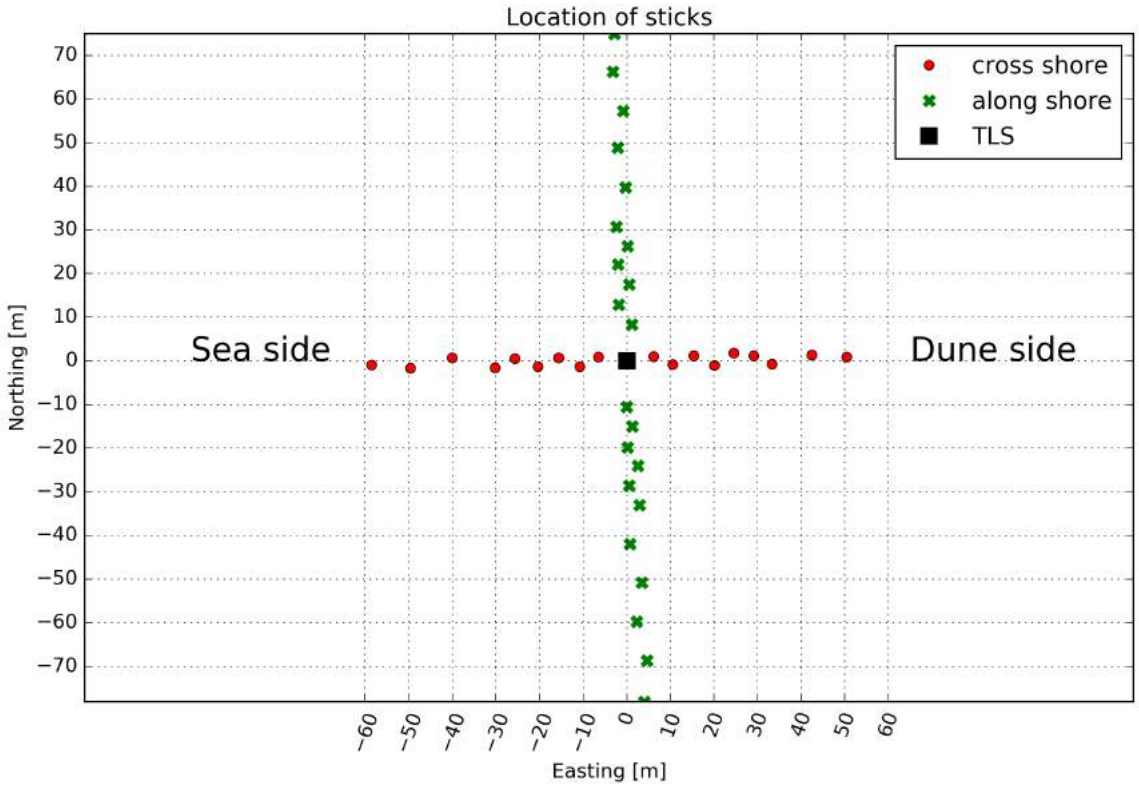

Figure A.1: Location of the sticks used to align TLS and GPS measurements, coordinates relative to TLS are used.

A.3. Results

The coordinates measured with the TLS are subtracted from the coordinates measured with GPS and these deviations are shown in figure A.2, A.3, A.4 and A.5. Easting and Northing are replaced with x and y coordinates respectively. A positive deviation means that the coordinate measured with GPS is bigger. The results are separated in along shore and cross shore direction. Multiple scan positions and one single scan position are separated within that direction segregation.

A.3.1. Along shore direction

In the along shore direction the deviation of x and y coordinates show an order of magnitude comparable to the GPS accuracy, for both single and multiple scan positions, see figure A.2 and A.3. The x coordinates measured by the TLS are closer to the GPS's coordinates than the y coordinates. However, their behavior is comparable; both slightly increase with range from the laser scanner or remain more or less constant. One solution for the scanners position shows more outliers are seen than with multiple scan positions, for both x and y.

The deviations in z coordinates measured in the alongshore direction increase with distance from the laser scanner, see figure A.2 and A.3. Remarkable are the positive bias of the deviations, for the z coordinates, and the smaller deviations with multiple scan positions.

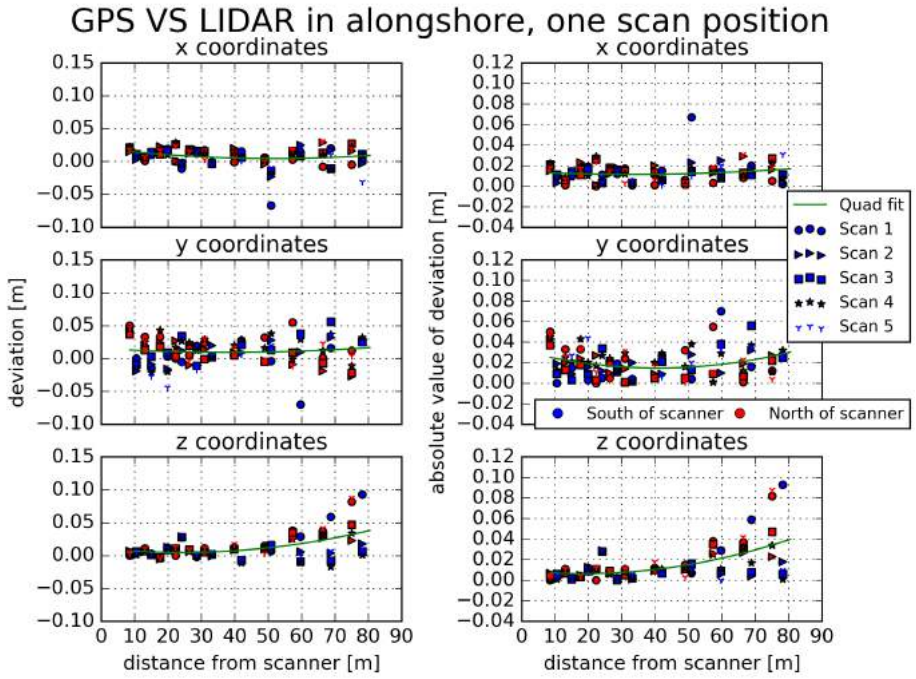

Figure A.2: GPS minus TLS measured coordinates in along shore direction. TLS measured coordinates are obtained with one single solution of the scanners position, thus one scan position.

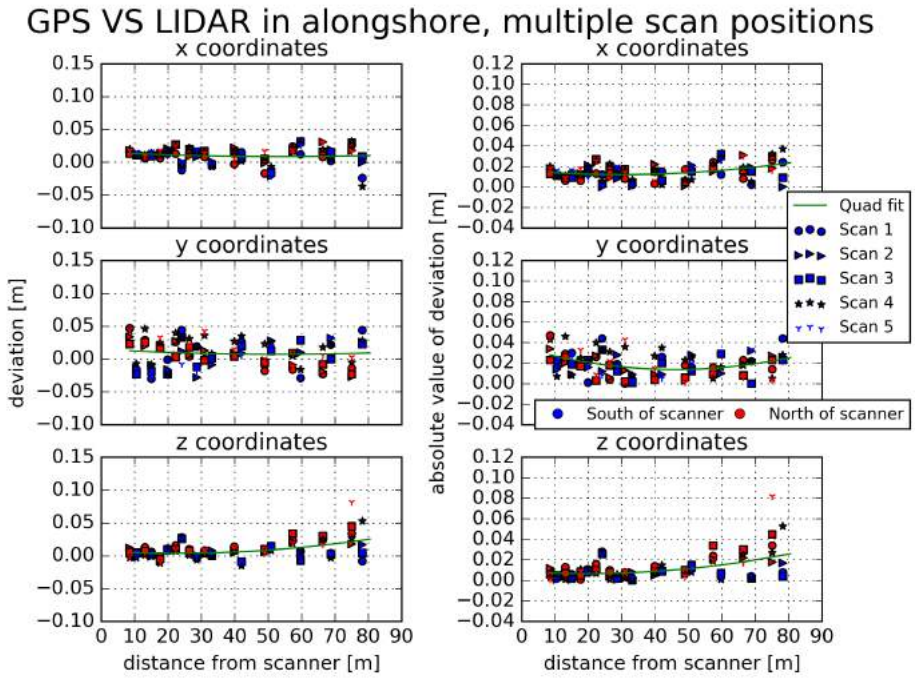

Figure A.3: GPS minus TLS measured coordinates in along shore direction. TLS measured coordinates are obtained with a solution of the scanners position for each individual scan, thus multiple scan positions.

A.3.2. Cross shore direction

The deviation of x and y coordinates show, similar to the along shore direction, an order of magnitude comparable to the GPS accuracy, for both the single and multiple scan positions in cross shore direction, see figure A.4 and A.5. Now the y coordinates measured with TLS are closer to the coordinates measured with GPS, instead of the x coordinates. The deviations in x coordinates become a little bit less if the distance from the laser scanner increases, but it is questionable whether this is significant since the trend seems to be smaller than the scatter of the points at larger distance. For the y coordinate is first an increase seen with distance and then a decrease.

In the onshore and offshore direction a distinction between the behaviors of the z coordinates can be made. It can be seen that the onshore deviations, in absolute value, increase slightly with distance and are then remain around an approximately constant level. For the off shore direction decreasing deviations can be seen. The above holds for both multiple scan positions and one scan position. In the cross shore direction a negative biased behavior can be seen. Decreasing deviation, in absolute value, with distance from the scanner is observed if on and offshore are averaged together, see figure A.4 and A.5.

The stick offshore of the scanner at 30 meter range has been run over by a truck halfway through the experiment; this explains the big deviations it gives at certain points.

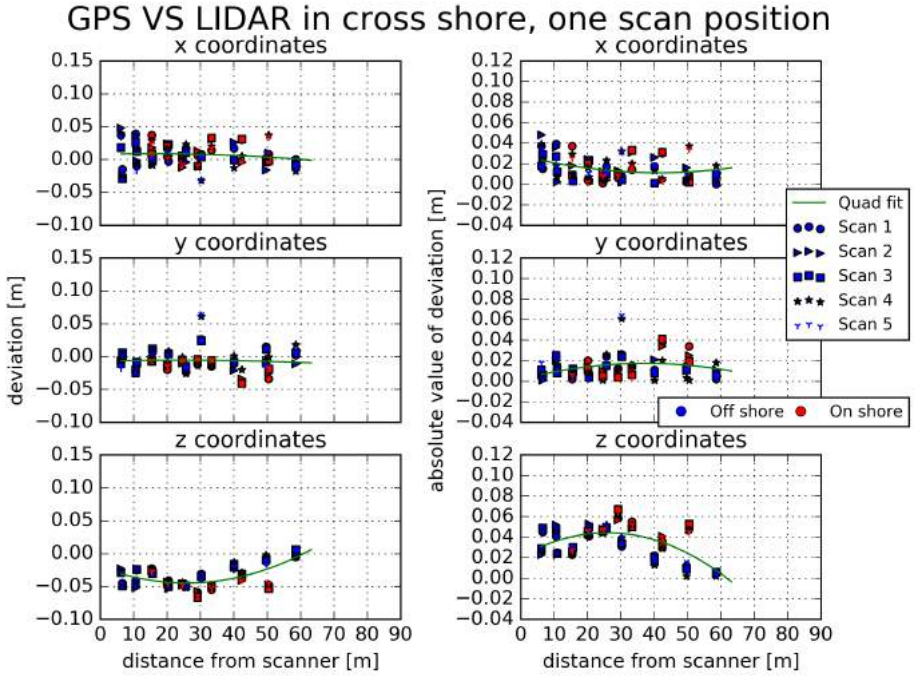

Figure A.4: GPS minus TLS measured coordinates in cross shore direction. TLS measured coordinates are obtained with one single solution of the scanners position, thus one scan position.

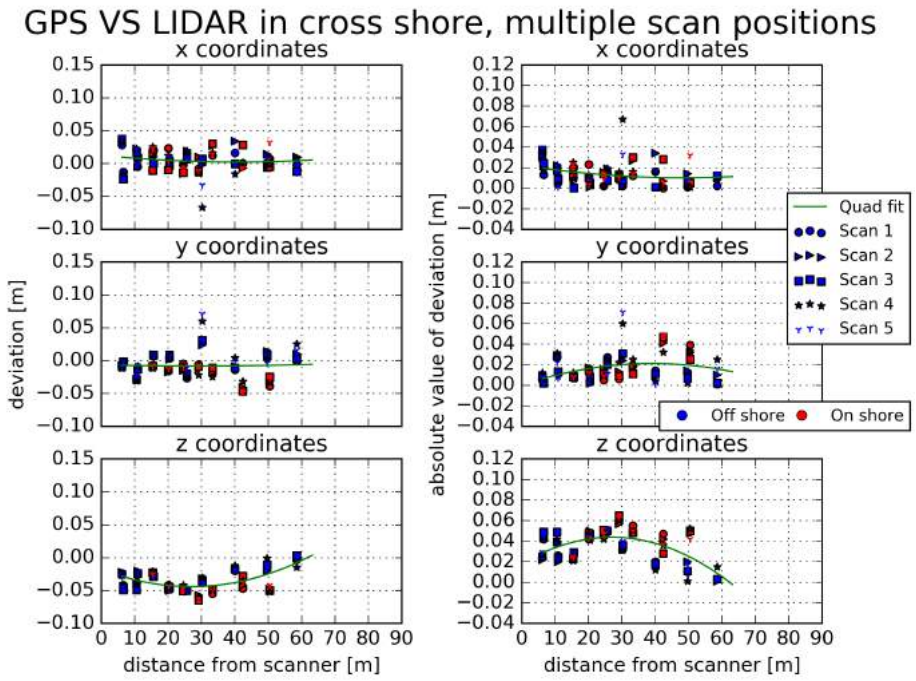

Figure A.5: GPS minus TLS measured coordinates in cross shore direction. TLS measured coordinates are obtained with a solution of the scanners position for each individual scan, thus multiple scan positions.

A.4. Discussion

Bigger deviations in x and y coordinates are seen, in paragraph A.3, for respectively cross and along shore direction. This is likely to occur due to combined effect of the x axis being mostly in along shore direction and y axis in cross shore direction and the method of selecting points in a 3D point cloud. Consider the situation with the x axis running through one of the sticks, so x axis perpendicular to stick front, and the y axis is perpendicular to x axis. A sharp transition, between a lot of points and no points, is seen in x direction due to the stick blocking the laser. This enforces less deviation in x coordinate, the point that needs to be chosen can be easily determined regarding the x direction. In y direction a point more or less in the middle of the stick is chosen. This can deviate more since no sharp transitions are seen in y direction.

Wet sand could be a reason for the different behavior between onshore and offshore in z coordinate deviations observed in the cross shore direction, see paragraph A.3. It is stated that in the cross shore direction a negative bias is seen for the deviations. In off shore direction the differences become more and more positive, which reduces the absolute deviations. In on shore direction the same behavior is seen the first couple of meters and then differences remain more or less constant. Wet sand could be a reason for this diverging behavior, due to high water the sand was wet more off shore of the scanner.

A.5. Conclusion

The main question for this appendix is “How do the observations done by the TLS compare to measurements done with GPS?”. The first sub question is “Are the deviations between TLS and GPS different in along shore direction with respect to the cross shore direction?”. “Does the difference between TLS and GPS increase with distance from the scanner?” is another sub question. The last one refers to the processing method “Are there differences between coordinates obtained with one and multiple scan positions?”. The hypothesis with these questions is that the deviations between TLS and GPS measured coordinates scatter around a certain value, comparable to the GPS accuracy, and then, at a certain distance from the scanner, start to increase with distance. This behavior is expected for both cross and along shore direction and for a single and multiple scan positions. It is thus not hypothesized that the direction and number of times the scanners position is determined influences the deviations between GPS and TLS measured coordinates.

The x and y coordinate deviations increase slightly or not at all with distance from the laser scanner, for both cross and along shore direction. The x coordinates vary more in the cross shore direction and y coordinates in along shore direction, due to the method of determining the TLS measured coordinates and the defined coordinate system, see paragraph A.4. Calculating the scanners position once, one scan position for all scans, or for every scan doesn't influence the deviations in x and y coordinates. Only a couple more outliers can be seen in the along shore direction with one scan position.

Differences in z coordinates behave differently in along shore and cross shore direction. They increase significant with range from the scanner for the along shore direction. This behavior is seen more with a single scan position than for multiple scan positions. A remarkable positive bias is seen in the along shore direction. In the cross shore direction a negative bias is seen. This means that in along shore direction the TLS measured coordinates are all smaller than the GPS measured coordinates, in the cross shore direction they are larger. In off shore direction the differences become more and more positive, same as in along shore direction, which reduces the absolute deviations. In on shore direction the same behavior is seen the first couple of sticks and then differences remain more or less constant for the last few. The reason for the diverging behavior could be the moisture content of the soil.

Overall can be concluded that deviations from the GPS measurements are in the order of centimeters, especially up to 50 meter range from the scanner.

A.6. Recommendations

The method that is now used gives different deviations for x and y coordinate if the x and y axis are oriented differently. Therefore it deserves recommendation to do the same test again but with a different way of determining the points that are measured with GPS in the scan of the TLS. This could maybe be done by making squares of material that absorbs the laser and placing them in the same fashion as the reflective sticks. This will give in the 3D point cloud a border of no points around the point that is measured with GPS.

In this research no reason could be thought of to explain the positive bias in along shore direction and the negative bias in cross shore direction. Doing another research can reveal whether this behavior is real and could give more insight in what caused these biases, since this is only the result of one experiment.

B

Windless day

B.1. Introduction

"What are the results on a day without wind obtained with the adopted processing routine and scanner use?" is the main question for this appendix. The important results are the trend, correlation coefficient and standard deviation. The differences between a single and multiple scan positions are also looked into for these results. One scan position means that the position of the scanner is once determined using the ground control points (GCP's), see paragraph 2.3 for more explanation, and this position is used for every scan. Multiple positions mean that this is done for every scan individually.

The hypothesis is that the trend should be very small with a low corresponding correlation coefficient and the observed standard deviation should be small as well. This should be the case for both single and multiple scan positions. For multiple scan positions the standard deviation should be a bit bigger.

B.2. Methodology

Thirteen scans are done on 17 August 2016 with an interval of 7.5 minutes. The wind was almost absent that day, see figure B.1. These scans are processed and analyzed as is done for the windy days, see paragraph 2.3.2.

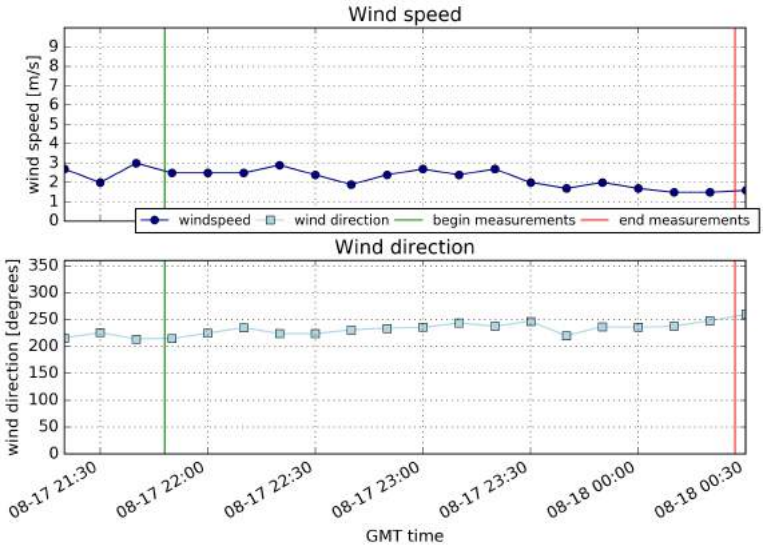

Figure B.1: Wind speed and wind direction as measured on the 17th of August at the SEDEX² measurement site.

B.3. Results

The observed trend is not zero for both a single scan position and multiple scan positions, see figure B.2. A bigger trend is seen for the single position case. With this more significant trend also higher correlation coefficients, r^2 values, are found. The standard deviation of both methods are in the same order of magnitude, millimeters up to a centimeter, only a bit bigger in the upper left corner for multiple positions and lower right corner for single position.

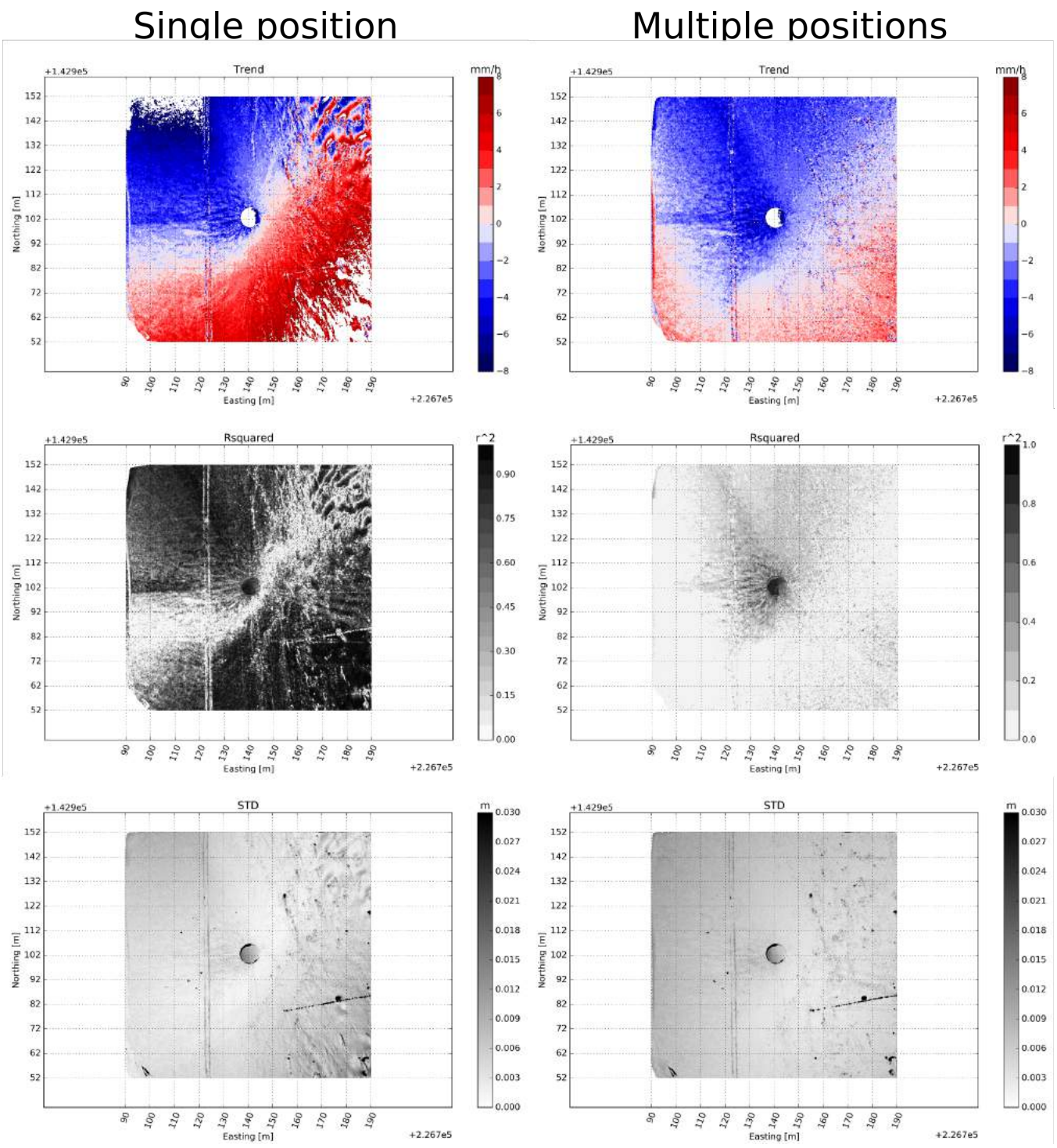

Figure B.2: Results, trend, correlation coefficient and standard deviation, for single and multiple scanner positions. Single position is on the left and multiple positions right.

B.4. Discussion

Subsidence of one of the tripod's legs could explain the trend that is observed for the single scan position. It has approximately an axis that runs straight through the laser scanner, see figure B.2. This axis is also perpendicular to one of the tripod's legs in the set-up for this sequence. The laser beam needs to travel shorter on the side of the scanner where one of the legs lowers, see figure B.3. This causes an increase in measured heights at that side of the scanner, because a faster return will mean that the scanner thinks the measured point is higher. On the other side lower values will be measured, the laser's return time is longer.

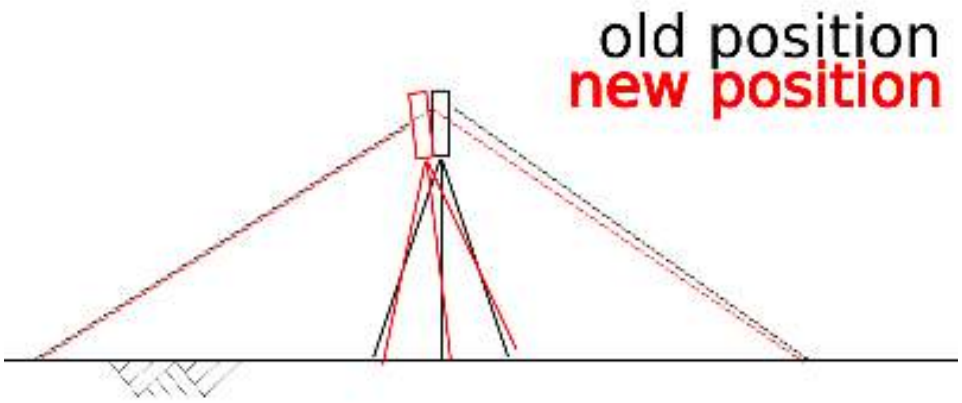

Figure B.3: Subsidence of one of the tripod's legs and influence on distance laser beams have to travel to reach the ground.

Using multiple positions should remove the fake trend caused by settling of one of the tripod's legs, assuming that the GCP's do not move. The scanners position is calculated for every individual scan and thus subsidence should be taken into account. However, this solution still shows a trend, see figure B.2. The trend for multiple positions is bigger left of the scanner than right. It also shows a higher standard deviation in the upper left corner of the domain. These observations could be explained by the fact that the GCPs were located closer to the scanner at the left side and that this side had fewer GCP's, causing a larger degree of freedom for the solution on the left of the scanner. This is visualize in figure B.4 for a case with two GCPs. GCP A is located further away from the TLS than GCP B. This means that the deviation of the solution in A will be a bit larger than the solution in B. The deviation is a summation of TLS inaccuracies and GPS inaccuracies and is therefore not necessary linear increasing with the range, see also appendix A. Using the extremes of these deviations gives two solution planes, 1 and 2. It can be seen that the deviation between the solution planes on the right is bigger than in A due to the fact that GCP A is located further away than GCP B.

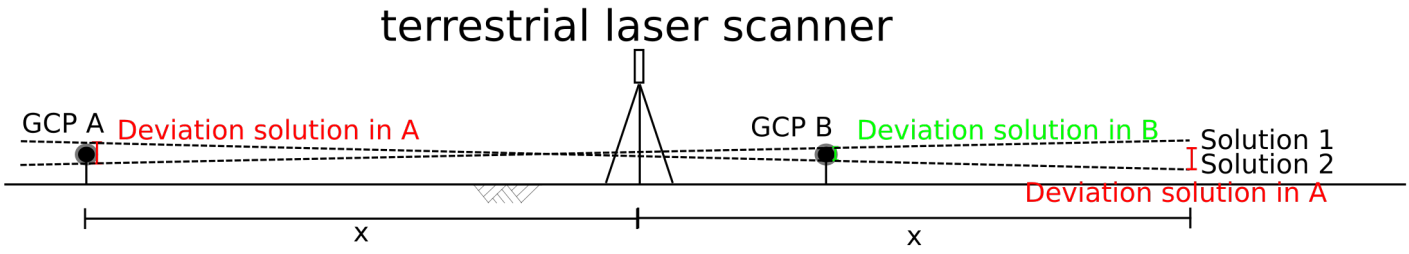

Figure B.4: Two different solutions for the TLS location in a 2D plane with the placement of 2 GCP's. The deviation in measured bed elevations at distance x right from the scanner is bigger than left of the scanner, in A.

B.5. Conclusion

The main question for this appendix is “What are the results on a day without wind, due to adopted processing routine and scanner use?”. The important results are the trend, correlation coefficient and standard deviation. The differences between a single and multiple scan positions are also looked into for these results. It was hypothesized that the observed trend would be very small with a low corresponding correlation coefficient and the observed standard deviation would be small as well, for both single and multiple scan positions.

Paragraph B.3 shows that the observed trend is not zero for both a single solution and multiple solutions for the scanners position. The multiple positions case shows a smaller trend. Also the correlation coefficient of this solution makes more sense, it is near zero. The standard deviations of both methods are approximately the same, except in the upper left corner and lower right. Using multiple solutions for the scanners position works better, based on the summary above. Caution is required by interpreting this method, since it still shows a trend the correlation coefficient is important.

B.6. Recommendations

The location of the GCP’s could be the cause of the higher trend on the left of the scanner, with respect to the right, in case of multiple scan positions, see paragraph B.4. Therefore it is recommended for future scans that the GCP’s are placed further away from the scanner on the left and the number of GCP’s is increased.

Another recommendation is that the scans are analyzed by using multiple solutions for the scanners positions, since that came out more trustworthy, see paragraph B.5

C

Wind during measuring campaign

During the SEDEX² measuring campaign the wind speed and wind direction are measured in the middle of the research area on top of a dune. Figure C.1 shows the wind speed as measured during the whole topographic measurement campaign. In figure C.2 is zoomed in on the periods of the TLS measuring sequences to show some more details.

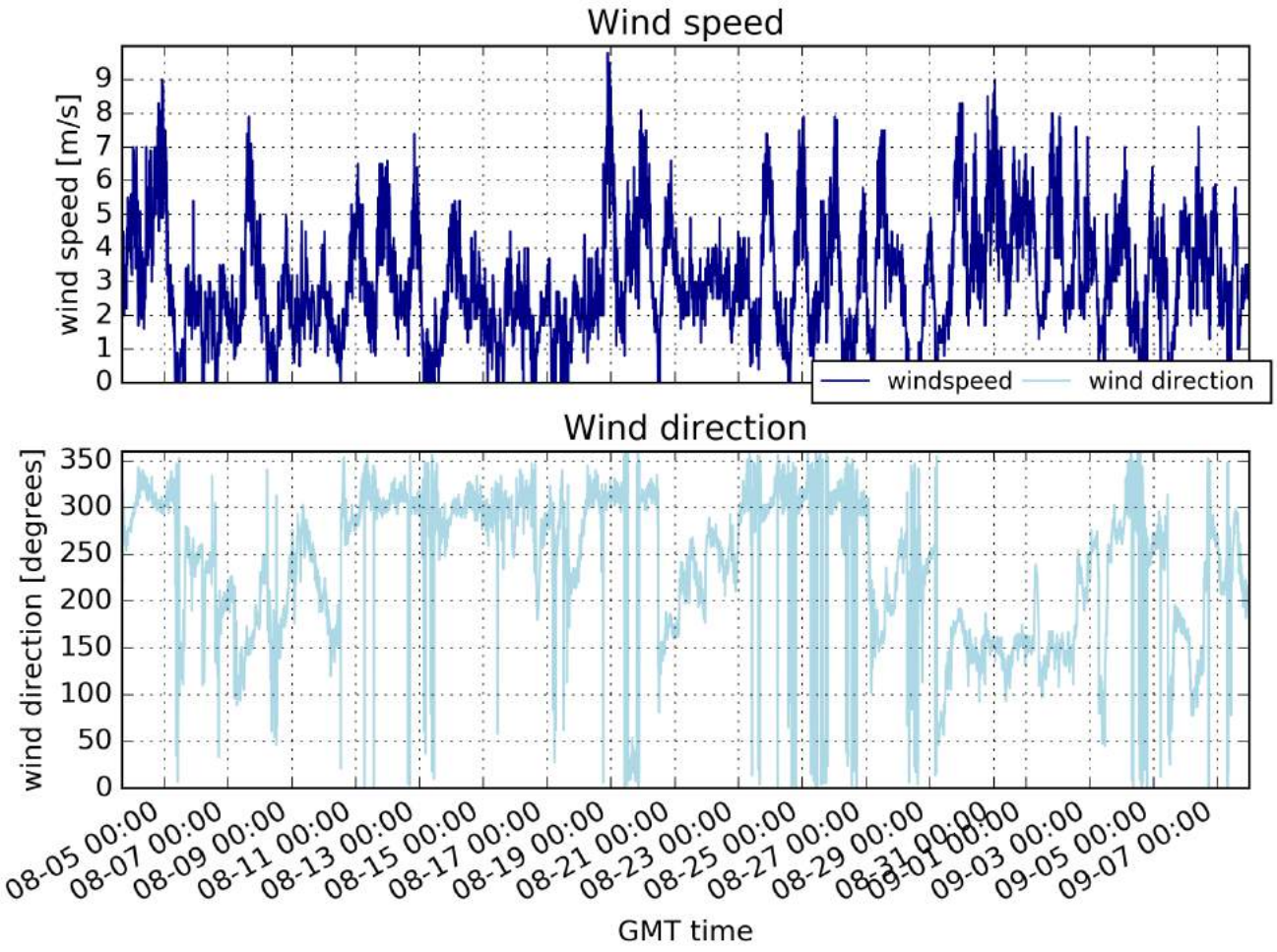

Figure C.1: Wind as measured during measuring campaign in the SEDEX² area, from 08-02-2016 to 08-09-2016.

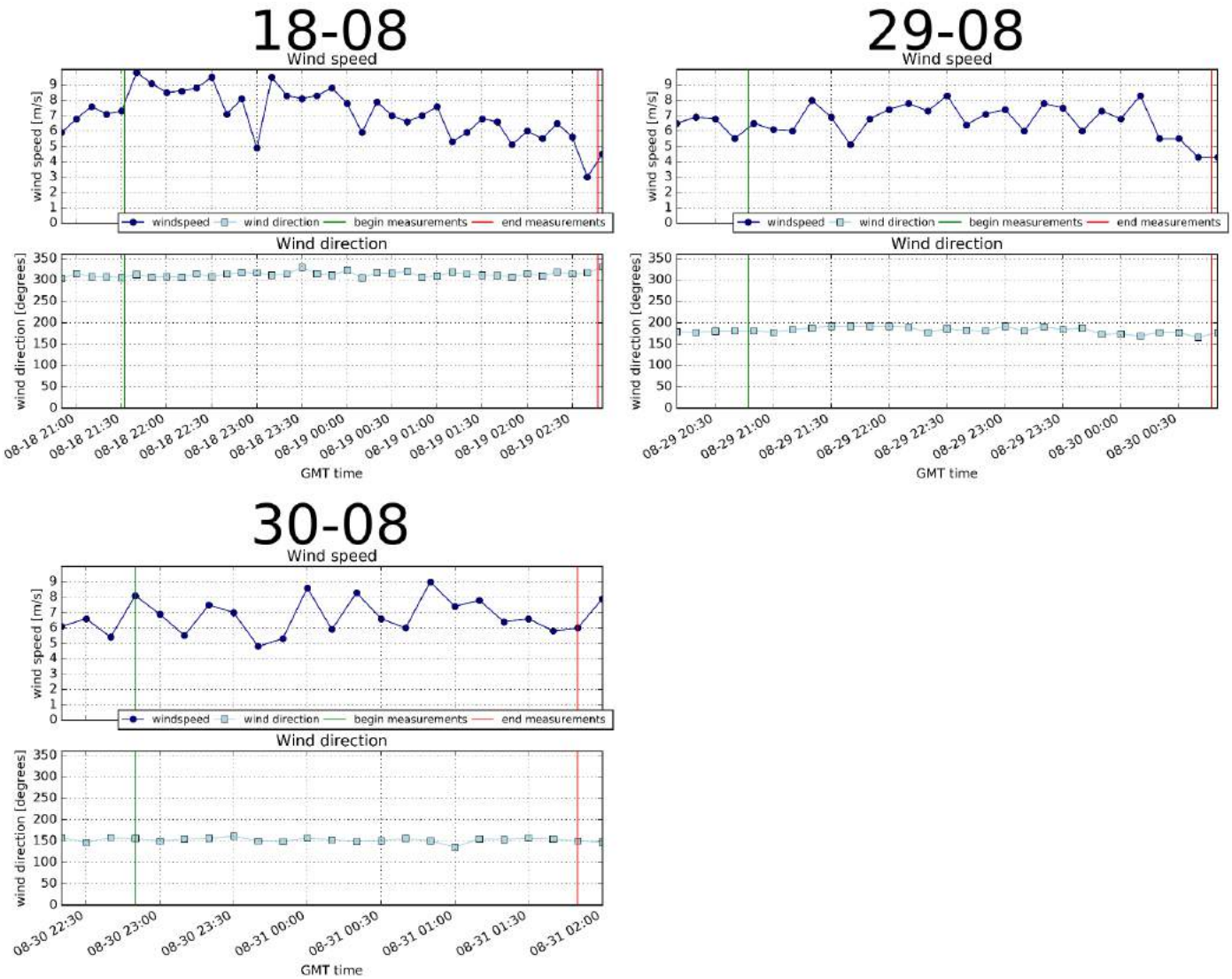

Figure C.2: Wind speed and wind direction as measured during the TLS measuring sequences in the SEDEX² area.

D

Tidal signal

The tidal signal at Toke Point WA, measured by the National Oceanic and Atmospheric Administration [NOAA], is used in combination with an estimation of run-up, set-up and swash to approximate the height of the water line in the TLS area. The run-up, set-up and swash on top of this tidal signal is computed with the wave data measured outside Grays Harbor by the NOAA [national data bouycenter] and the formulas proposed by Stockdon [2006]. These formulas are:

$$R_2 = <\eta> + \frac{S}{2}$$

$$<\eta> = 0.35 * \beta_f * \sqrt{H_0 * L_0}$$

$$S = \sqrt{S_{inc}^2 + S_{ig}^2}$$

$$S_{inc} = 0.75 * \beta * \sqrt{H_0 * L_0}$$

$$S_{ig} = 0.06 * \sqrt{H_0 * L_0}$$

$With$:

$R_2 = run\ up\ exceeded\ by\ 2\%\ of\ the\ time$ [m]

$H_0 = offshore\ significant\ wave\ height\ (measured\ with\ bouy)$ [m]

$L_0 = offshore\ wave\ length = \frac{g * T_0^2}{2 * \pi}$ [m]

$T_0 = offshore\ wave\ period\ (measured\ with\ bouy)$ [s]

$\beta_f = slope\ of\ foreshore = estimated\ at\ \frac{2.6}{150}$ [$-$]

Using the formulas above and adding the measured tide gives the signal as shown in figure D.1. Note that this is still just an approximation since the tide is measured in a bay and the waves are measured offshore at a different location. This signal is also not for the complete topographic measurement period because the wave data wasn't free available that far back in time.

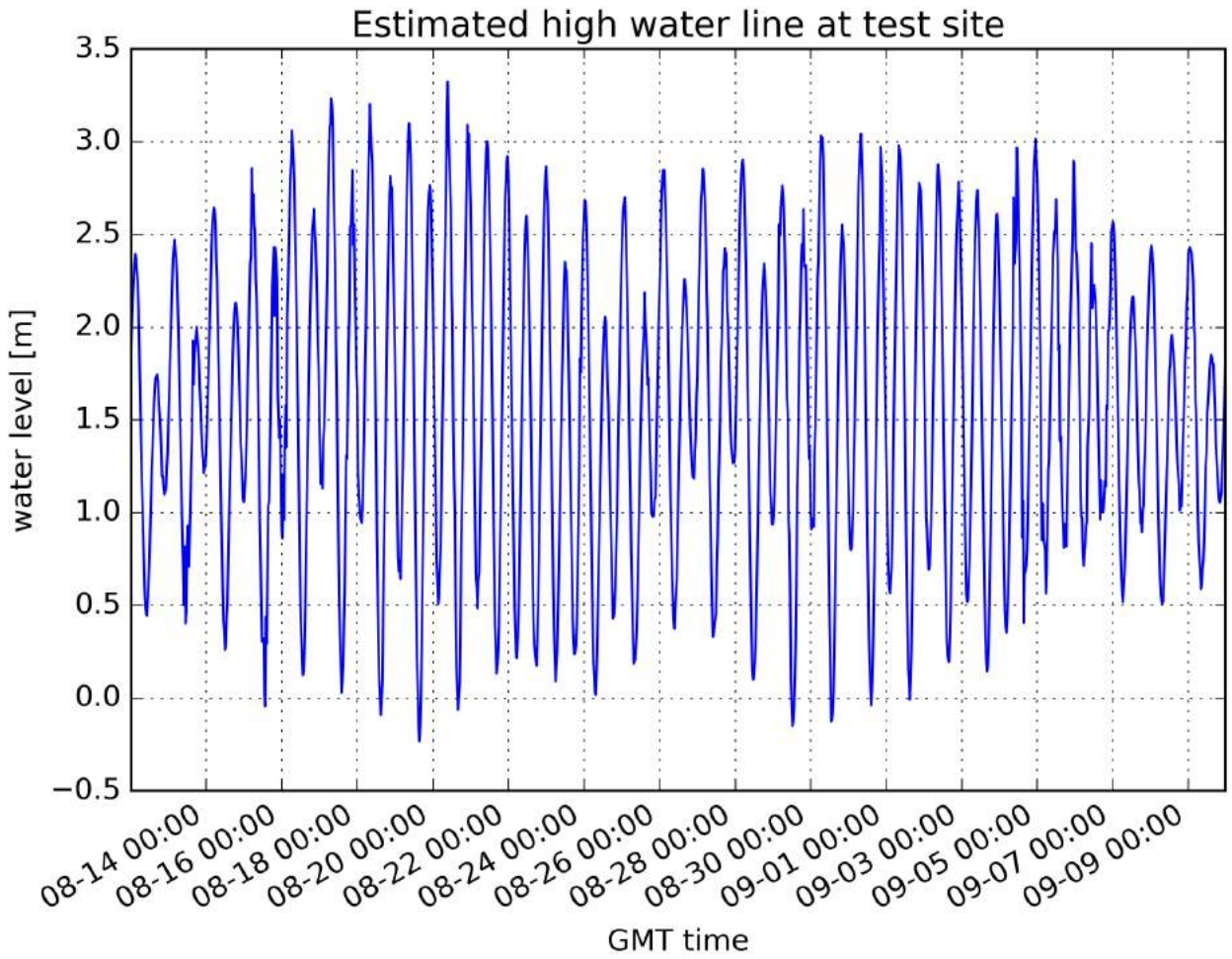

Figure D.1: Tidal signal after adding run-up, set-up and swash to the tidal signal measured at Toke Point.